Clin Orthop Relat Res (2013) 471:2484–2491
DOI 10.1007/s11999-013-2809-x

Clinical Orthopaedics and Related Research®
A Publication of The Association of Bone and Joint Surgeons®

SYMPOSIUM: ADVANCED HIP ARTHROSCOPY

Novel CT-based Three-dimensional Software Improves the Characterization of Cam Morphology

Michael T. Milone BA, Asheesh Bedi MD, Lazaros Poultsides MD, PhD, Erin Magennis BA, J. W. Thomas Byrd MD, Christopher M. Larson MD, Bryan T. Kelly MD

Published online: 30 January 2013

Abstract

Background Incomplete correction of femoral offset and sphericity remains the leading cause for revision surgery for symptomatic femoroacetabular impingement (FAI). Because arthroscopic exploration is technically difficult, a detailed preoperative understanding of morphology is of paramount importance for preoperative decision-making.

Questions/purposes The purposes of this study were to (1) characterize the size and location of peak cam deformity with a prototype CT-based software program; (2) compare software alpha angles with those obtained by plain radiograph and CT images; and (3) assess whether differences can be explained by variable measurement locations.

Methods We retrospectively reviewed the preoperative plain radiographs and CT scans of 100 symptomatic cam lesions treated by arthroscopy; recorded alpha angle and clockface measurement location with a novel prototype CT-based software program, CT, and Dunn lateral plain radiographs; and used ordinary least squares regressions to assess the relationship between alpha angle and measurement location.

Results The software determined a mean alpha angle of 70.8° at 1:23 o'clock and identified 60% of maximum alpha angles between 12:45 and 1:45. The CT and plain radiographs underestimated by 5.7° and 8.2°, respectively. The software-based location was anterosuperior to the mean CT and plain radiograph measurement locations by 41 and 97 minutes, respectively. Regression analysis confirmed a correlation between alpha angle differences and variable measurement locations.

Conclusions Software-based three-dimensional (3-D) imaging generated alpha angles larger than those found by plain radiograph and CT, and these differences were the result of location of measurement. An automated 3-D assessment that accurately describes the location and topography of FAI may be needed to adequately characterize preoperative deformity.

Level of Evidence Level III, diagnostic study. See the Guidelines for Authors for a complete description of levels of evidence.

One or more of the authors certifies that he (JWTB, CML, BTK) has or may receive payments or benefits, during the study period, an amount of USD 10,000–USD 100,000, from A^2 Surgical (Saint-Pierre-d'Allevard, France). None of the other authors have received any payments or benefits related to this project. All ICMJE Conflict of Interest Forms for authors and *Clinical Orthopaedics and Related Research* editors and board members are on file with the publication and can be viewed on request. Each author certifies that his or her institution approved the human protocol for this investigation, that all investigations were conducted in conformity with ethical principles of research, and that informed consent for participation in the study was obtained. This work was performed at the Hospital for Special Surgery, New York, NY, USA.

M. T. Milone
University of Pennsylvania, Philadelphia, PA, USA

A. Bedi
University of Michigan, Ann Arbor, MI, USA

L. Poultsides, E. Magennis, B. T. Kelly
Hospital for Special Surgery, New York, NY, USA

J. W. T. Byrd
Nashville Sports Medicine Foundation, Nashville, TN, USA

C. M. Larson (✉)
Twin Cities Orthopaedics, 4010 West 65th Street, Edina, MN 55435, USA
e-mail: chrislarson@tcomn.com

Introduction

Loss of femoral offset secondary to a cam deformity can result in hip impingement and shear forces of the femoral head against the acetabulum and secondary acetabular chondral delamination, degenerative changes of labrum, hip pain, and osteoarthritis of the hip [1, 2, 4, 7–9, 11, 13, 15–18, 20–23, 29, 32]. Although cam lesions can be surgically corrected with arthroscopic or open osteoplasty [8, 10, 26], failure to completely correct femoral offset and sphericity remains the leading cause for revision surgery for symptomatic femoroacetabular impingement (FAI) [30]. Open surgery has the advantage of complete intraoperative visualization of the impingement region, but arthroscopic assessment of residual impingement after decompression can be limited in particular for extreme ROM positions. Thus, accurate preoperative planning is needed to determine the location for decompression, and improved imaging may ultimately yield improved arthroscopic surgical corrections.

In the preoperative assessment of FAI, abnormal femoral morphology has been quantified by measures of head sphericity and head-neck offset. The alpha angle, first described by Notzli et al. [27], is defined as the angle between the femoral neck axis and a line connecting the center of the femoral head to the point of commencement of femoral head asphericity [3]. The alpha angle correlates with preoperative symptoms and cam lesion size [1, 34] and is additionally used postoperatively to assess the achieved surgical correction [18, 19].

Plain radiography [7, 24, 33], CT [6], and MRI [15, 24, 27, 28, 31] have all been used to assess FAI. Although an alpha angle measurement of greater than 50° on the commonly used frog lateral radiograph is reportedly 90.9% specific for FAI, the frog lateral is less sensitive than both AP and Dunn lateral views because its clinical use is limited to the identification of anterior femoral deformities [25]. Meyer et al. [24], in a comparison of six radiographic projections, suggested the Dunn lateral radiography was the most accurate plain radiograph technique to characterize the cam deformity, and this view has been validated by Barton et al. [5] with a sensitivity 91%, specificity 88%, positive predictive value of 93%, negative predictive value of 84%, and accuracy of 90% compared with MRI. However, a number of authors have suggested circumferential assessment on radial images identifies substantially larger alpha angles than their axial counterparts by arguing that a two-dimensional (2-D) radiograph or an isolated axial cross-sectional image that is not orthogonal to the region of maximal deformity may fail to identify and/or underestimate the size of the femoral deformity [3, 6, 15, 24, 28]. Nepple et al. [25], in a review of 41 hips, show that alpha angle correlation between plain radiograph and CT is dependent on the location of radial imaging, suggesting that differences may reflect the variable location of measurement along the circumference of the head-neck junction.

We (1) use a novel, prototype CT-based three-dimensional (3-D) analysis software tool to describe the alpha angles and clockface locations of peak cam deformity; (2) compare software alpha angle measurements with additional measurements obtained from modified Dunn lateral plain radiograph and CT imaging studies; and (3) assess whether differences in alpha angles can be explained by differences in location of measurement.

Patients and Methods

We conducted a nonconsecutive retrospective case series assessing the preoperative imaging of 50 male and 50 female patients, mean age 29 years old (range, 16–55 years old), who underwent primary arthroscopic osteoplasty from August 2010 to July 2011 for symptomatic FAI by the senior author (BTK) at the single study institution. All patients with preoperative standardized Dunn lateral plain radiographs and high-resolution CT studies obtained at the study institution were eligible. During the study time, a total of 378 hips were treated by osteoplasty for primary FAI. Of these, 219 met the inclusion criteria, and all excluded patients had one of the required imaging studies performed at an outside institution not attainable for study review. Sixty-eight hips, 41 male and 27 female, were initially selected based on the presence of DICOM CT images on compact discs, because these were required for loading into the prototype software used in the study. An additional 32 hips were blindly selected from a deidentified list of included patients containing no information on previously recorded alpha angles or hip pathology. To report sex differences, a balance between female and male hips was sought, and because adequate imaging on 41 male hips was already obtained, a total of 100 hips consisting of 50 male and 50 female hips were targeted. At completion, 100 hips from 91 patients were enrolled, none of which had revisions or required revision. This study was approved by our institutional review board.

AP pelvis Dunn radiographs, captured at one facility with an average radiation dose of 0.7 mSv, were standardized when taken to confirm symmetry of the obturator foramina and central location of the coccyx 1.5 to 2 cm above the pubic symphysis. The extended-neck lateral (Dunn) radiograph was obtained with the hip in 90° of flexion and the femur in 20° of abduction and 0° of rotation [24]. The x-ray beam was angled 15° in the AP direction to be tangential to the acetabular plane and centered on the femoral shaft approximately 6 cm lateral to the anterosuperior iliac spine.

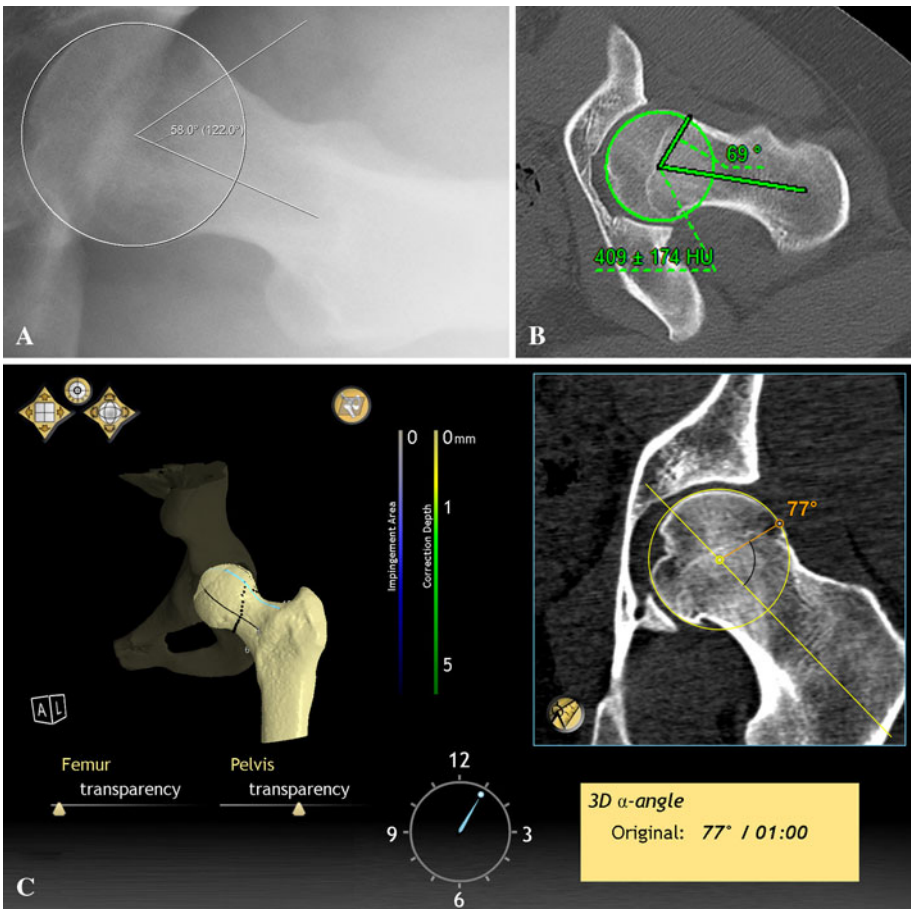

Fig. 1A–C All images depict a hip of the same patient. (**A**) Dunn lateral plain radiograph recording an alpha angle of 58° at 3:00 on the femoral head-neck junction. (**B**) Conventional CT measurement of 69° at 2:00. (**C**) CT-based 3-D software recording 77° at 1:00.

From the Dunn lateral plain radiographs, alpha angles were measured by a single fellowship-trained orthopaedic surgeon (LP). Clockface nomenclature was used for localization of the maximum cam deformity at the femoral head-neck junction with the superior location of the lateral epiphyseal vessels designated as 12 o'clock. All alpha angles were measured in a plane orthogonal to the radiographic beam at the anterior head-neck junction approximating the 3 o'clock location. The alpha angle was defined as the angle subtended between the midline of the femoral neck and a line connecting the center of the femoral head to the point along the head-neck junction that first deviates from the sphericity of the femoral head (Fig. 1A). The intraobserver and interobserver variability of Dunn lateral alpha angle measurement has been described at R = 0.98 and R = 0.90, respectively [24]. To reduce potential observer bias toward underestimation of alpha angles, measurements were recorded at 2× magnification and any judgments of ambiguous asphericity favored the larger alpha angle calculation.

With a 64-channel CT scanner, high-resolution CT scans were taken with bone acquisition and standard reformatting algorithms set to 0.625-mm slice thickness retrospectively reconstructed from 2.5 mm, 512 × 512 resolution, and average dose of 200 mA at 0.5 seconds with a pitch of 1.375, which gives an approximate dose length product of 150 to the hip and 50 to the knee. This technique, combined with Adaptive Statistical Iterative Reconstruction, a dose-lowering algorithm designed by GE Healthcare (Waukesha, WI, USA) that lowers radiation dose by an additional 20%, equates to 2.85 mSv at the hip and 0.075 mSv to the knee. The average 2010 Medicare reimbursement for CT of the hip was $241.73 (Current Procedural Terminology 73700), and the settings used in this study were performed at no additional cost to the patient. To keep the lower extremities still during the scan, the patient's feet were turned inward toward each other and taped together. One of two fellowship-trained musculoskeletal radiologists (GD, DD) with greater than 11 years of experience in evaluating hip CTs reviewed these scans because in clinical practice, radiologists, and not the attending orthopaedic surgeon, record and report the data of interest to this study. The radiologists measured alpha angles from a series of 2-D radial reconstructions across the femoral neck axis with the aforementioned alpha angle measurement technique (Fig. 1B). To minimize variation in measurements dependent on the angle subtended along the femoral neck, images were reviewed by board-certified radiologists (GD, DD) before interpretation to confirm that data sets were reconstructed parallel with the center of the femoral neck for

both oblique axial images as well as in the rotation view. The radiologists then used clinical judgment to determine the clockface location of the maximum cam deformity to the nearest 15th minute, resulting in four possible locations per clockface hour. Femoral torsion was also measured as the angle subtended between the femoral neck and the posterior condylar axis. The center of the neck was defined by multiaxial radial sequences to define the central axis in the superoinferior, mediolateral, and AP planes, and the posterior condylar axis was described by axial images of the distal femur. Recently, Heyworth et al. [14], when assessing the CT measurements of GD and DD (along with two additional radiologists not used in this study), described the interrater reliability for alpha angle and femoral version measurements with intraclass correlation coefficients of 0.72 and 0.94, respectively.

A prototype CT-based, 3-D analysis computer software program (A^2 Surgical, Saint-Pierre-d'Allevard, France) was used to measure alpha angles from the high-resolution CT images (this prototype software is still in development and has not been cleared for clinical use by the FDA or any other regulatory body). For each patient, a DICOM-formatted CT was loaded to generate image series displaying axial and coronal views of the femoral head on which a computer-generated best fit sphere was created with the capacity for manual adjustment. Accounting for all clockface possibilities at 15-minute increments, the program then uses an automated algorithm based on radial sequences to determine the maximum alpha angle and its location (Fig. 1C), because radial sequencing provides the most accurate assessment of femoral head asphericity, decreased offset, and circumferential alpha angle assessment around a 360° sphere [3, 6, 15, 24, 28]. The software identifies the center of the femoral neck and calculates the 2-D alpha angle at multiple points around the sphere of the femoral head at 15° increments. Thus, 24 discreet alpha angles are calculated around the sphere of the femoral head, and the greatest alpha angle value and location is identified and automatically reported. Scrolling around the sphere, with a calculated measurement at each 15th degree, the remaining circumferential alpha angles are readily identified at these intervals. An orthopaedic surgeon (LP) reviewed the software image to confirm the plausibility of the computer-determined location. This surgeon (LP) then manually set the software's measurement location to that previously determined as the location of CT alpha angle measurement, and the software provided an additional alpha angle at this location. For further comparison to CT, the software also determined the femoral torsion for all hips involved in this study in a method identical to that of the CT.

Mean plain radiograph, CT, and computer-generated alpha angle measurements and locations were calculated for males and females. Differences in alpha angles among plain radiograph, CT, and software were determined using a repeated-measures analysis of variance (ANOVA) applying Box's conservative epsilon and post hoc Bonferroni-corrected paired t-tests. To assess the relationship between alpha angle differences and locations of measurement, we determined differences in location of measurement among plain radiograph, CT, and software using the same statistical analyses. We further described alpha angle differences between imaging modalities as a function of lesion clockface location by using variants of the following simple ordinary least squares (OLS) regression:

$$\text{MeasurementDiff}_i = \beta_1 \text{LocationDiff}_i + \varepsilon_i \quad (1)$$

where the dependent variable, MeasurementDiff, is the difference in the alpha angle measurement determined by two imaging modalities for Patient i, and the independent variable, LocationDiff, is the difference in the maximum alpha angle location determined by these same two imaging modalities for Patient i. For any two imaging modalities, β_1, the coefficient on LocationDiff, can be interpreted as the degree difference in alpha angle that occurs for every hour of clockface difference in measurement location. To maintain positive values for and ease the interpretation of this coefficient, the imaging modality with the smaller mean alpha angle was always subtracted from the imaging modality with the larger mean alpha angle when describing MeasurementDiff_i. The data met the linearity, independence, homoscedasticity, and normality assumptions of a simple linear regression. We then used paired t-tests to determine differences in CT alpha angles and software alpha angles recorded when the software was manually overridden to measure at the clockface location of CT measurement. We also determined differences in femoral torsion measurements between software and CT using paired t-tests to further assess whether distorted software reconstruction could contribute to discrepancies. We used Stata Statistical Software: Release 11 (StataCorp LP, College Station, TX, USA) to analyze the data.

Results

The mean alpha angle calculated by the CT-based prototype software was 70.8° (74.4° for males, 67.2° for females; range, 45.0°–95.0°) (Table 1), and the mean location of peak deformity was the 1:23 o'clock position along the femoral head-neck junction. Sixty percent of cam lesions were largest between 12:45 and 1:45 (Fig. 2).

Repeated-measures ANOVA revealed differences between both alpha angles ($F[2, 198] = 33.39$, $p < 0.001$) and measurement locations ($F[2, 198] = 230.95$, $p < 0.001$) determined by software, CT, and plain radiograph. The software alpha angle was larger ($p < 0.001$) (Table 2) than both the mean radiologist-based CT alpha angle of 65.1°

Table 1. Summary statistics of alpha angles, lesion locations, and femoral torsions (N = 100; 50 male, 50 female)

Variable	Mean ± SD
Age (years)	29.1 ± 9.8
Male	28.0 ± 9.6
Female	30.1 ± 1.4
Software alpha angle (degrees)	70.8 ± 10.7
Male	74.4 ± 11.6
Female	67.2 ± 11.6
CT alpha angle (degrees)	65.1 ± 10.3
Male	69.7 ± 7.4
Female	60.5 ± 10.9
Plain radiograph alpha angle (degrees)	62.6 ± 11.6
Male	67.6 ± 10.8
Female	57.6 ± 10.3
Software alpha angle at CT location (degrees)	64.4 ± 10.5
Male	68.3 ± 9.2
Female	60.4 ± 10.3
Software lesion location (clockface)	1:23 ± 0:43
Male	1:20 ± 0:41
Female	1:26 ± 0:46
CT lesion location (clockface)	2:04 ± 0:45
Male	1:59 ± 0:50
Female	2:10 ± 0:39
CT torsion (degrees)	15.8 ± 7.9
Male	15.9 ± 8.4
Female	15.6 ± 7.5
Software torsion (degrees)	16.3 ± 7.9
Male	15.3 ± 8.1
Female	17.3 ± 7.7

(69.7° for males, 60.5° for females; range, 33.0°–84.0°) and the mean plain radiograph alpha angle of 62.6° (67.6° for males, 57.6° for females; range, 30.5°–85.0°) (Table 1) by 5.7° and 8.2°, respectively. The radiologist CT alpha angle was also larger ($p = 0.0495$) than that measured on plain radiographs (Table 2). Although locations were recorded at 15-minute intervals, mean location was calculated, and the software mean lesion location of 1:23 o'clock was 41 minutes anterosuperior ($p < 0.001$) to the mean location of 2:04 o'clock based on the CT review and 97 minutes anterosuperior ($p < 0.001$) to the approximate Dunn lateral plain radiograph lesion location of assessment at 3:00 (Table 2). The CT location was 56 minutes anterosuperior ($p < 0.001$) than the Dunn lateral (Table 2). Regression analysis revealed the Dunn lateral radiograph and traditional CT underestimated the magnitude of asphericity relative to the software ($p < 0.001$) by 6.0°/clockface hour ($\beta_1 = 6.0$) and 4.6°/clockface hour ($\beta_1 = 4.6$), respectively (Table 3). As the lesion location determined by CT deviated further from 3:00, the CT alpha angle exceeded that of the plain radiograph by 4.3°/clockface hour ($\beta_1 = 4.3$, $p = 0.002$) (Table 3). The mean software-determined alpha angle

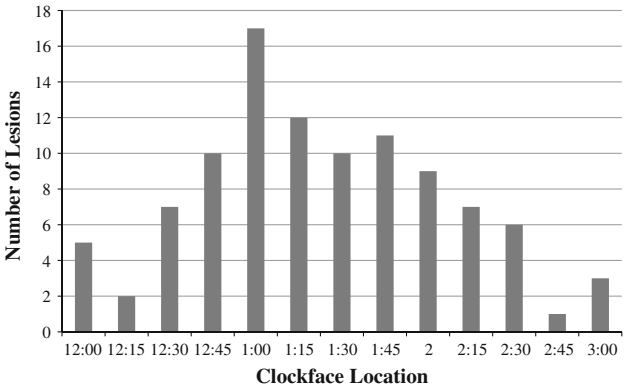

Fig. 2 Bar graph details the number of study patients with maximum lesion locations at each corresponding 15-minute clockface interval as determined by CT software. The most common maximum lesion location was 1:00 with 17 patients presenting at this location. Sixty of 100 patients presented with maximum lesions between 12:45 and 1:45, and only three had maximum lesions at 3:00.

Table 2. Paired t-tests comparing alpha angles, lesion locations, and femoral torsions

Alpha angle	Larger modality or sex	Difference (degrees)	p value
Software versus CT	Software	5.7	< 0.001*
Software versus Dunn lateral	Software	8.2	< 0.001*
CT versus Dunn lateral	CT	2.5	0.0495*
Software at CT location versus CT	CT	0.7	0.15
Male versus female			
By software	Male	7.1	< 0.001
By CT	Male	9.1	< 0.001
By Dunn lateral	Male	10	< 0.001
Lesion location	**Antero-superior modality**	**Difference (clockface hours)**	**p value**
Software versus CT	Software	0:41	< 0.001†
Software versus Dunn lateral	Software	1:37	< 0.001†
CT versus Dunn lateral	CT	0:56	< 0.001†
Femoral torsion	**Larger modality**	**Difference (degrees)**	**p value**
Software versus CT	Software	0.54	0.16

Asterisk and dagger denote post hoc Bonferroni-adjusted p values after repeated-measures analysis of variance: *$F(2, 198) = 33.39$, $p < 0.001$; †$F(2, 198) = 230.95$ $p < 0.001$.

Table 3. Ordinary least squares regression accounting for lesion location

Modalities compared	Mean Measurement Diff	Mean Location Diff	β_1 degrees/ clockface hour
Software-CT	5.7°	0:41	4.6 ($t = 3.65$, $p < 0.001$)
Software-plain radiograph	8.2°	1:37	6.0 ($t = 4.62$, $p < 0.001$)
CT-plain radiograph	2.5°	0:56	4.3 ($t = 3.23$, $p = 0.002$)

(64.4°) was similar to ($p = 0.15$) the CT alpha angle when measured at the matched clockface locations (Table 2). Similarly, the measured femoral torsion based on CT (15.8°) was similar to ($p = 0.16$) the software-determined femoral torsion (16.3°) (Tables 1, 2).

Discussion

Arthroscopic treatment of FAI has grown exponentially, and the most common reason for failure is incomplete bony resection [30]. Because arthroscopic assessment of impingement can be limited, a detailed preoperative understanding of the volume, location, and topography of the cam deformity is of paramount importance. The purposes of this study are to (1) use a prototype CT-based software tool to describe the size and location of symptomatic cam lesions; (2) compare software alpha angle measurements with those obtained from plain radiograph and CT images; and (3) assess whether differences in alpha angles can be explained by differences in locations of measurement.

This study is not without limitations. First, this study assumes the prototype software accurately quantifies alpha angles and locations of peak cam deformity, but the software tool has not been validated against cadaveric specimens. However, three-dimensional imaging is the gold standard for detection of femoral head-neck deformity [6, 31], and we found no differences in CT and software femoral torsion or alpha angle measurements controlled for location, suggesting that the software provides an accurate interpretation of CT images. Second, the software is only capable of quantifying cam pathology with alpha angles at 15-minute intervals along the head-neck junction, and radiologists reported locations of measurement to the same precision. This renders software maximum alpha angle measurements marginally conservative, and, in the extreme and unlikely scenario that the radiologists misreported every measurement location posteroinferiorly by 15 minutes, a 25-minute measurement difference between CT and software would remain and the related β_1 would not be affected. Third, because inclusion criteria included preoperative plain radiograph and CT images, there may be selection bias toward patients with underwhelming cam lesions on the Dunn lateral. However, the study institution's workup routinely includes both imaging studies, and all operative patients had both imaging tests. Fourth, one of us (LP) recorded a single set of plain radiograph alpha angles, and this author's measurements may have been universally conservative. This author (LP) mitigated this potential bias with methods described, and the plain radiograph alpha angles are consistent with existing literature (Table 4). Fifth, the presumed location of measurement by plain radiograph is based on the assumption of a perfect Dunn lateral, but the image may be performed with variable precision depending on the technician. To minimize this variability, all radiographs were standardized when taken.

By describing the size and location of cam lesions in a review of 100 symptomatic hips, this study provides valuable information for preoperative planning of arthroscopic osteoplasty for FAI. Consistent with previously reported measurements (Table 4), the mean alpha angle was 70.8°, and males (74.4°) presented with larger alpha angles than females (67.2°) [1, 3, 27, 34]. The average location of a symptomatic cam lesion's peak deformity was

Table 4. Previous studies determining alpha angles with Dunn radiographs or radial imaging

Study	Dunn alpha angle	Radial alpha angle	Radial location	Number
Barton et al. [5]	61			68
Meyer et al. [24]	65			11
Nepple et al. [25]	57.2	59.8 (CT)	1:00–2:00	41
Beaule et al. [6]		66.4 (CT)	12:00–2:00	30
Domayer et al. [12]		65.2 (MR)	Superoanterior	60
Pfirrmann et al. [28]		68 (MR)	Anterosuperior	50
Rakhra et al. [31]		70.5 (MR)	1:00–2:00	41
Current study	62.6	70.8 (software)	12:45–1:45	100
		65.1 (CT)	1:30–2:30	

at 1:23; 17% of lesions generated maximum alpha angles at 1:00, and 60% were largest between 12:45 and 1:45. This localization reaffirms the anterosuperior prevalence found in smaller studies [6, 12, 25, 28] describing the location of maximum deformity by radial imaging (Table 4). Only 3% of lesions were best appreciated at 3:00 (Fig. 2), a finding of critical importance, because the Dunn lateral radiograph obtained in the current study imaged the 3:00 location in profile and missed the peak of the cam deformity along the anterosuperior head-neck junction.

The plain radiograph and CT alpha angles underestimate the magnitude of deformity compared with software analysis by 8.2° and 5.7°, respectively. The 8.2° of Dunn lateral underestimation is a unique finding, because prior studies directly comparing alpha angles obtained by Dunn radiography with 3-D imaging find less discrepancy [5, 25]; however, Barton et al. [5] compares the Dunn radiograph with axial imaging, which has been consistently described as inferior to radial assessments [3, 6, 15, 24, 28], and Nepple et al. [25] determined small alpha angles (59.8°) by CT, possibly because they aggregate data from 41 hips, of which only 56% contained isolated cam type impingement. Because three-dimensional imaging is considered the gold standard for assessment of FAI [6, 31], no prior study has questioned CT-derived alpha angles by comparison to bone specimens. Regardless, a quantitative underestimation of cam deformity by CT can be overcome if the surgeon explores the more important qualitative information provided by the 3-D image. However, a single radiograph provides less information, and, although underestimation on Dunn lateral or any plain film may not alter the decision to operate, it may generate an inaccurate assessment of lesion extent.

The plain radiograph and CT measured alpha angles at 3:00 and 2:04, respectively, which are 97 and 41 minutes different from the mean of 1:23 determined by computer-assisted software. The OLS regression analysis further revealed that these variable locations of measurement contribute to the relative alpha angle underestimation, because the CT and Dunn lateral underestimated alpha angle size by 4.6° and 6.0°/clockface hour of location error, respectively (Table 3). Furthermore, the CT software analysis tool was no different than the radiologist-based CT measurements when accounting for clockface location (Table 1). This implies that differences in alpha angle measurement can be attributed to differences in location of measurement. Our regression analysis specifically suggests the Dunn lateral underestimates alpha angles because it projects images profile to the 3:00 anterior location, but prior studies [5, 23] have found the Dunn view is most useful for the assessment of anterosuperior cam lesions. The reason for this is unclear, and further investigation is needed. If measurements of head-neck offset are to be made on plain radiographs, the pursuit of a novel technique for capturing a profile image of the common anterosuperior location of peak deformity found in this study may be warranted. Nonetheless, the dependency of the alpha angle on the location of measurement, combined with the variable locations of cam deformity described in this study, renders any plain radiograph, restricted to measurement in the plane of the film, limited in its ability to quantify FAI. We therefore support the use of 3-D imaging in the assessment of FAI. Because CT is capable of assessment at any clockface location, we suspect the inaccurate CT location observed in this study may reflect an observer bias to assess toward the traditional anterior location. This suggests radiologists must not hesitate to deviate from measuring the alpha angle at the 3:00 position described by Notzli et al. [25] on cross-sectional CT or MR studies and should rather assess radial sequences in multiple planes to assure that the peak of the deformity has been captured. This task can be facilitated by a 3-D tool that circumferentially assesses the head-neck junction, thereby improving the preoperative characterization of deformity that is paramount to the long-term success of an arthroscopic hip preservation procedure for FAI.

In conclusion, we used a novel CT-based software to characterize symptomatic cam lesion size and location. We found that this software recorded larger alpha angles than both CT and Dunn lateral plain radiographs and that these differences can be explained by differences in measurement location. Because of the variable location of cam lesions, the three-dimensional software system that automatically performs a circumferential assessment of the femoral head-neck junction may be useful for preoperative characterization of FAI.

Acknowledgments We thank Stephane Lavalle and Laurence Chabanas for their assistance with the prototype CT-based three-dimensional analysis software tool. We thank Douglas Decorato, MD, and Gavin Duke, MD, for their contributions to the CT protocol and measurements.

References

1. Allen D, Beaule PE, Ramadan O, Doucette S. Prevalence of associated deformities and hip pain in patients with cam-type femoroacetabular impingement. *J Bone Joint Surg Br.* 2009;91:589–594.
2. Anderson LA, Peters CL, Park BB, Stoddard GJ, Erickson JA, Crim JR. Acetabular cartilage delamination in femoroacetabular impingement. Risk factors and magnetic resonance imaging diagnosis. *J Bone Joint Surg Am.* 2009;91:305–313.
3. Banerjee P, McLean CR. Femoroacetabular impingement: a review of diagnosis and management. *Curr Rev Musculoskelet Med.* 2011;4:23–32.
4. Bardakos NV, Villar RN. Predictors of progression of osteoarthritis in femoroacetabular impingement: a radiological study with a minimum of ten years follow-up. *J Bone Joint Surg Br.* 2009;91:162–169.

5. Barton C, Salineros MJ, Rakhra KS, Beaule PE. Validity of the alpha angle measurement on plain radiographs in the evaluation of cam-type femoroacetabular impingement. *Clin Orthop Relat Res*. 2011;469:464–469.
6. Beaule PE, Zaragoza E, Motamedi K, Copelan N, Dorey FJ. Three-dimensional computed tomography of the hip in the assessment of femoroacetabular impingement. *J Orthop Res.* 2005;23:1286–1292.
7. Beck M, Kalhor M, Leunig M, Ganz R. Hip morphology influences the pattern of damage to the acetabular cartilage: femoroacetabular impingement as a cause of early osteoarthritis of the hip. *J Bone Joint Surg Br*. 2005;87:1012–1018.
8. Bedi A, Chen N, Robertson W, Kelly BT. The management of labral tears and femoroacetabular impingement of the hip in the young, active patient. *Arthroscopy.* 2008;24:1135–1145.
9. Bedi A, Dolan M, Leunig M, Kelly BT. Static and dynamic mechanical causes of hip pain. *Arthroscopy.* 2011;27:235–251.
10. Bedi A, Zaltz I, De La Torre K, Kelly BT. Radiographic comparison of surgical hip dislocation and hip arthroscopy for treatment of cam deformity in femoroacetabular impingement. *Am J Sports Med.* 2011;39(Suppl):20S–28S.
11. Clohisy JC, Carlisle JC, Trousdale R, Kim YJ, Beaule PE, Morgan P, Steger-May K, Schoenecker PL, Millis M. Radiographic evaluation of the hip has limited reliability. *Clin Orthop Relat Res.* 2009;467:666–675.
12. Domayer SE, Ziebarth K, Chan J, Bixby S, Mamisch TC, Kim YJ. Femoroacetabular cam-type impingement: diagnostic sensitivity and specificity of radiographic views compared to radial MRI. *Eur J Radiol*. 2011;80:805–810.
13. Guanche CA, Bare AA. Arthroscopic treatment of femoroacetabular impingement. *Arthroscopy*. 2006;22:95–106.
14. Heyworth BE, Dolan MM, Nguyen JT, Chen NC, Kelly BT. Preoperative three-dimensional CT predicts intraoperative findings in hip arthroscopy. *Clin Orthop Relat Res*. 2012;470: 1950–1957.
15. Ito K, Minka MA 2nd, Leunig M, Werlen S, Ganz R. Femoroacetabular impingement and the cam-effect. A MRI-based quantitative anatomical study of the femoral head-neck offset. *J Bone Joint Surg Br*. 2001;83:171–176.
16. Johnston TL, Schenker ML, Briggs KK, Philippon MJ. Relationship between offset angle alpha and hip chondral injury in femoroacetabular impingement. *Arthroscopy.* 2008;24:669–675.
17. Kelly BT, Weiland DE, Schenker ML, Philippon MJ. Arthroscopic labral repair in the hip: surgical technique and review of the literature. *Arthroscopy.* 2005;21:1496–1504.
18. Konan S, Rayan F, Haddad FS. Is the frog lateral plain radiograph a reliable predictor of the alpha angle in femoroacetabular impingement? *J Bone Joint Surg Br*. 2010;92:47–50.
19. Larson CM, Giveans MR. Arthroscopic management of femoroacetabular impingement: early outcomes measures. *Arthroscopy*. 2008;24:540–546.
20. Leunig M, Beck M, Kalhor M, Kim YJ, Werlen S, Ganz R. Fibrocystic changes at anterosuperior femoral neck: prevalence in hips with femoroacetabular impingement. *Radiology*. 2005;236: 237–246.
21. Leunig M, Beck M, Woo A, Dora C, Kerboull M, Ganz R. Acetabular rim degeneration: a constant finding in the aged hip. *Clin Orthop Relat Res.* 2003;413:201–207.
22. Mardones R, Gonzalez C, Chen Q, Zobitz M, Kaufman KR, Trousdale RT. Surgical treatment of femoroacetabular impingement: evaluation of the effect of the size of the resection. Surgical technique. *J Bone Joint Surg Am.* 2006;88(Suppl 1):84–91.
23. Mardones R, Lara J, Donndorff A, Barnes S, Stuart MJ, Glick J, Trousdale R. Surgical correction of 'cam-type' femoroacetabular impingement: a cadaveric comparison of open versus arthroscopic débridement. *Arthroscopy*. 2009;25:175–182.
24. Meyer DC, Beck M, Ellis T, Ganz R, Leunig M. Comparison of six radiographic projections to assess femoral head/neck asphericity. *Clin Orthop Relat Res.* 2006;445:181–185.
25. Nepple JJ, Martel JM, Young-Jo K, Zaltz I, Clohisy JC. Do plain radiographs correlate with CT for imaging of cam-type femoracetabular impingement. *Clin Orthop Relat Res.* 2012;470: 3313–4420.
26. Ng VY, Arora N, Best TM, Pan X, Ellis TJ. Efficacy of surgery for femoroacetabular impingement: a systematic review. *Am J Sports Med.* 2010;38:2337–2345.
27. Notzli HP, Wyss TF, Stoecklin CH, Schmid MR, Treiber K, Hodler J. The contour of the femoral head-neck junction as a predictor for the risk of anterior impingement. *J Bone Joint Surg Br.* 2002;84:556–560.
28. Pfirrmann CW, Mengiardi B, Dora C, Kalberer F, Zanetti M, Hodler J. Cam and pincer femoroacetabular impingement: characteristic MR arthrographic findings in 50 patients. *Radiology*. 2006;240:778–785.
29. Philippon MJ, Kuppersmith DA, Wolff AB, Briggs KK. Arthroscopic findings following traumatic hip dislocation in 14 professional athletes. *Arthroscopy.* 2009;25:169–174.
30. Philippon MJ, Schenker ML, Briggs KK, Kuppersmith DA, Maxwell RB, Stubbs AJ. Revision hip arthroscopy. *Am J Sports Med.* 2007;35:1918–1921.
31. Rakhra KS, Sheikh AM, Allen D, Beaule PE. Comparison of MRI alpha angle measurement planes in femoroacetabular impingement. *Clin Orthop Relat Res*. 2009;467:660–665.
32. Robertson WJ, Kadrmas WR, Kelly BT. Arthroscopic management of labral tears in the hip: a systematic review of the literature. *Clin Orthop Relat Res.* 2007;455:88–92.
33. Tannast M, Siebenrock KA, Anderson SE. Femoroacetabular impingement: radiographic diagnosis—what the radiologist should know. *AJR Am J Roentgenol.* 2007;188:1540–1552.
34. Tanzer M, Noiseux N. Osseous abnormalities and early osteoarthritis: the role of hip impingement. *Clin Orthop Relat Res.* 2004;429:170–177.